University of Groningen

OmegaCAM and gravitational lensing

Christen, Fabrice Frédéric Thiébaut

IMPORTANT NOTE: You are advised to consult the publisher's version (publisher's PDF) if you wish to cite from it. Please check the document version below.

Document Version
Publisher's PDF, also known as Version of record

Publication date:
2007

Link to publication in University of Groningen/UMCG research database

Citation for published version (APA):
Christen, F. F. T. (2007). *OmegaCAM and gravitational lensing*. s.n.

Copyright
Other than for strictly personal use, it is not permitted to download or to forward/distribute the text or part of it without the consent of the author(s) and/or copyright holder(s), unless the work is under an open content license (like Creative Commons).

The publication may also be distributed here under the terms of Article 25fa of the Dutch Copyright Act, indicated by the “Taverne” license. More information can be found on the University of Groningen website: https://www.rug.nl/library/open-access/self-archiving-pure/taverne-amendment.

Take-down policy
If you believe that this document breaches copyright please contact us providing details, and we will remove access to the work immediately and investigate your claim.

Downloaded from the University of Groningen/UMCG research database (Pure): http://www.rug.nl/research/portal. For technical reasons the number of authors shown on this cover page is limited to 10 maximum.

Download date: 14-07-2024

4

CCD Charge Transfer Efficiency Derived From Signal Variance in Flat Field Images*

Based on F. Christen, K.Kuijken, D. Baade, C. Cavadore, S. Dieries, O. Iwert. Scientific Detectors for Astronomy 2005; eds. Beletic, J. E., Beletic, J. W., Amico, P., p. 543-548., 2005.

ABSTRACT — In this chapter a novel technique is described for estimating the charge transfer efficiency (CTE) of a charge coupled device (CCD). This technique uses the change in variance with CCD row or column in flat field images (CVF method), and the fact that imperfect charge transfer during a readout has a smoothing effect on the final image. Simulated and real images, acquired during the characterization of the OmegaCAM CCDs, have been used to test and validate this method. Results from the CTE calculations by e2v, ESO and the results obtained with the variance based technique, developed in this chapter, are compared for nine CCDs. The outcome is promising and shows that this method can be used for simple and efficient CTE computations.

4.1 Introduction

The charge transfer efficiency (CTE) became a particularly important issue as CCD dimensions increased. Transporting charges from pixels, which are at the opposite side of the output port of the CCD without loosing electrons is very challenging particularly when one has to shift packets ~4100 times in the vertical direction and ~2000 times towards the output register, i.e. the 4k × 2k 44-82 e2v CCDs which compose the mosaic of the OmegaCAM camera (Kuijken et al., 2002). Specific procedures have been developed to obtain the efficiency of such a transfer. Two of them have been exploited and reported in the test protocol of the OmegaCAM CCDs, namely, the extended pixel edge response (EPER) method and a technique based on a radioactive source, ^{55}Fe (Janesick, 2001). The EPER method has to be used with caution because it is known to overestimate the CTE (Janesick, 2001) and to give sometimes poor unrealistic results with a CTE larger than 1.0 (Cavadore, 2000). The ^{55}Fe radioactive sources require specific official authorization and a special handling. We propose here an attractive alternative approach using only flat field images, we can compute the CTE with a higher precision than that of the EPER method by studying the variance of the number of electrons across the images.

To test the new method, we employ simulated images and flat images that have been taken to check the cosmetics of the OmegaCAM CCDs (Christen et al., 2004). Furthermore, we also describe how to use real images to determine the charge transfer efficiency with the Change in Variance in Flat-field (CVF) method.

After a brief description of the charge transfer efficiency in Section 4.2, the tools used to compute it are presented in Section 4.3. The popular extended pixel edge response (EPER) method is described (Sub-section 4.3.1) as well as our CVF method (Sub-section 4.3.2). Sub-section 4.3.3 explains how to reduce the data in order to extract the necessary information for applying the CVF method and sub-section 4.3.4 shows the impact of the CTE on the determination of the gain. In Section 4.4 are presented our first results from simulated and real data. A comparison with the EPER and the ^{55}Fe methods is also carried out.

4.2 Charge Transfer Efficiency, Definition.

After collecting the light during the integration period, the charges collected by each pixel have to be transfered to the output well. During the transfer, some charges are delayed due to the imperfection of the process. Defects in the silicon can remove a fraction of the charges from the transfered packet. The CTE is the parameter that characterizes the efficiency of the CCD to transfer correctly charges from one pixel to its neighbor pixel. An example of the effect of an imperfect CTE can be found in Figure 4.1.

In astronomy, applications require an excellent CTE. The minimum requirement is 0.999995 for both vertical and horizontal transfer. This number has to be very close to 1.0 not to degrade the quality of the image during the transfer of charges. With the OmegaCAM CCDs, which have a matrix of 4k by 2k pixels, the maximum deferred charge is, in theory, of about 3% of the total charge present in a pixel, if we take the minimum number of 0.999995 for parallel and perpendicular transfers.

4.3 The Methods

4.3.1 Extended Pixel Edge Response Method

To characterize the OmegaCAM CCDs, the EPER technique has been employed. To use this method, flat field images with overscan regions are necessary. The overscan regions are obtained by reading extra lines (columns) during the reading of the CCD (see Figure 4.2).

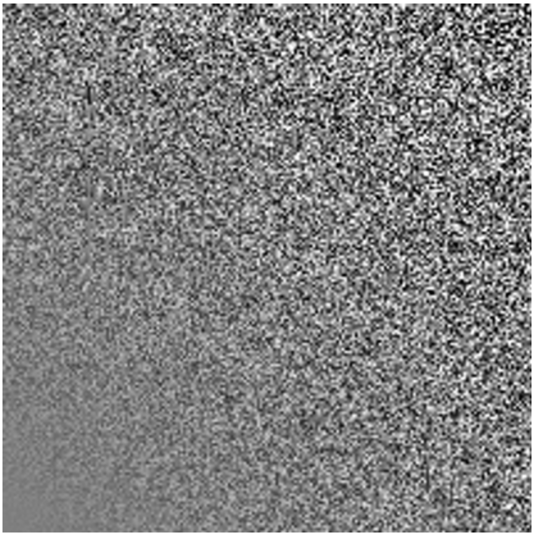

Figure 4.1: This image shows the effect of an imperfect CTE. A simulated flat field image (1k x 1k) has been created, duplicated and modified with a CTE equals to 0.999970. Figure 4.1 illustrates the remaining noise ("salt and pepper" pattern) one can observe after subtracting the modified flat field image from the original image. The changes in the pattern are visible at most far from the readout port which is located at the bottom left of this image.

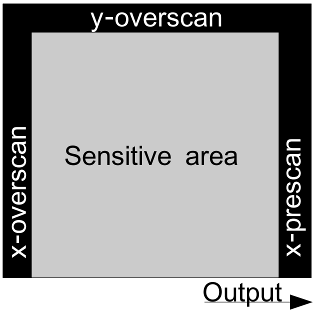

Figure 4.2: Example of an image with pre- and overscan regions. The prescan region stands for the pixels that are read before those of the sensitive area are read, the overscan region stands for the pixels that are read after those of the sensitive area are read.

The pre- and overscan regions in the case of the OmegaCAM CCDs are a result of the reading of extra pixels in the output register (for x-prescan and x-overscan) and the reading of extra lines for the y-overscan. The y-overscan region corresponds to the first 100 lines of the sensitive area obtained after reading the image recorded in the sensitive area. In all cases, the pixels values read in the pre- and overscan regions correspond to the bias level.
The delayed charges, due to the imperfect horizontal and vertical CTE, are collected in the x- and y-overscan, the majority of them is located in the first column and first line in those regions, respectively.

Consider a line of pixels with the output register on the right. In each pixel the number of electrons, N_e, is the same. Due to a charge transfer inefficiency almost all the charges in a pixel are shifted to the pixel on the right except a small fraction of electrons which remains in the former pixel. We have,

$$
\begin{array}{ccccccc|c}
\multicolumn{7}{c}{\text{Line of pixels with electrons}} & \text{Output Pixel} \\
\hline
 & \multicolumn{6}{c}{\text{Before shifting the charges}} & \\
 & N_e & N_e & N_e & \dots & N_e & N_e & 0 \\
 & \multicolumn{6}{c}{\text{After one shift to the right}} & \\
 & bN_e & N_e & N_e & \dots & N_e & N_e & aN_e \\
 & \multicolumn{6}{c}{\text{After two shifts to the right}} & \\
 & b^2N_e & b\,(1+a)\,N_e & N_e & \dots & N_e & N_e & aN_e \\
\sim & 0 & 2bN_e & N_e & \dots & N_e & N_e & N_e \\
 & \vdots & & & \vdots & & \vdots & \vdots \\
 & \multicolumn{6}{c}{\text{After } n \text{ shifts to the right}} & \\
\sim & 0 & 0 & 0 & \dots & 0 & nbN_e & N_e
\end{array}
$$

where N_e is the number of electrons, a is the Charge Transfer Efficiency (CTE), b is the Charge Transfer Inefficiency (CTI, $b = 1 - a$) and n is the total number of transfers necessary to read all the pixels.

After a complete transfer has taken place, we can express the number of charges left in the line of pixels due to an imperfect CTE as follows,

$$I_n = N_e \tag{4.1}$$

$$I_{n+1} = nbN_e \tag{4.2}$$

where I_n is the number of electrons in the last pixel of the sensitive area and I_{n+1} is the number of electrons left in the first pixel of the overscan region.

The charge transfer efficiency, $a\,(= 1 - b)$, is obtained using Equation (4.1) and Equation (4.2).

$$a = 1 - \frac{I_{n+1}}{nI_n} \tag{4.3}$$

In an image with x (y) overscan regions we compute the average number of electrons in the last line (column) and the average number of electrons left in the first line (column) of the overscan region. Knowing the number of transfers necessary to read the complete image, we can compute the charge transfer efficiency using Equation (4.3).

4.3.2 Change in Variance in Flat Field (CVF) Method

As an alternative to the study of the loss of the number of electrons using the EPER method, we analyze the reduction of the variance of the number of electrons across the flat field images.

This analysis is carried out in the following manner. During the transfer of charges the flat field images are smoothed due to the delayed charges present among the pixels. We assume here that we work with an ideal CCD, which means that there is neither a loss of charges in traps nor bad columns. Under these conditions the number of electrons in the flat field images remains constant during the transfer of charges, but the variance of the number of electrons decreases from one line (column) to the other as soon as the CCD is read. This statement is verified by the following demonstration.

The scheme below illustrates the effect of an imperfect transfer on the variance of the number of electrons. In each pixel we have a constant average number of electrons, N_e, and because of the Poisson statistics, the variance, $\sigma_e^2 = N_e$.

	Line of pixels with electrons				Output Pixel
		Before shifting the charges			
Signal	N_e	N_e	...	N_e	0
Variance	N_e	N_e	...	N_e	0
		One shift to the right			
Signal	bN_e	aN_e+ $+bN_e$	... ...	aN_e+ $+bN_e$	aN_e
Variance	b^2N_e	a^2N_e $+b^2N_e$	... ...	a^2N_e $+b^2N_e$	a^2N_e
		Two shifts to the right			
Signal	b^2N_e	$2abN_e+$ $+b^2N_e$	... ...	a^2N_e+ $+2abN_e+$ $+b^2N_e$	$2abN_e+$ $+a^2N_e$
Variance	b^4N_e	$4a^2b^2N_e+$ $+b^4N_e$	... ...	a^4N_e+ $+4a^2b^2N_e+$ $+b^4N_e$	$4a^2b^2N_e+$ $+a^4N_e$

After n shifts to the right

$$\begin{array}{llllll|l}
\text{Signal} & b^nN_e & b^nN_e+ & \ldots & b^nN_e+ & & a^nN_e+ \\
 & & +\binom{n}{1}b^{n-1}aN_e & \ldots & +\binom{n}{1}b^{n-1}aN_e+ & & +\binom{n}{1}a^{n-1}bN_e+ \\
 & & & \ldots & +\ldots+ & & +\ldots+ \\
 & & & \ldots & +\binom{n}{n-1}ba^{n-1}N_e & & +\binom{n}{n-1}ab^{n-1}N_e \\
\text{Variance} & b^{2n}N_e & b^{2n}N_e+ & \ldots & b^{2n}N_e+ & & a^{2n}N_e+ \\
 & & +\binom{n}{1}^2b^{2n-2}a^2N_e & \ldots & +\binom{n}{1}^2b^{2n-2}a^2N_e+ & & +\binom{n}{1}^2a^{2n-2}b^2N_e+ \\
 & & & \ldots & +\ldots+ & & +\ldots+ \\
 & & & \ldots & +\binom{n}{n-1}^2b^2a^{2n-2}N_e & & +\binom{n}{n-1}^2a^2b^{2n-2}N_e
\end{array}$$

From this scheme we can deduce that the variance, $\sigma_e^2(i)$, of each pixel in the line (column), i, follows the equation,

$$\begin{aligned}
\sigma_e^2(i) &= a^{2i}N_e + \binom{i}{1}^2 a^{2i-2}b^2N_e + \ldots + \binom{n}{n-1}^2 a^2b^{2n-2}N_e && (4.4)\\
&= a^{2i}N_e + \mathcal{O}(b^2) && (4.5)\\
&\approx N_e - 2ibN_e + \mathcal{O}(b^2) && (4.6)
\end{aligned}$$

where (b^2) is the residual, $\mathcal{O}(b^2) << a^{2i}N_e$.

Next, we express Equation (4.6) in Analogic Digital Units (ADU) instead of e^-. The average number of electrons, N_e, and the photon noise given by the standard deviation σ_e, measured in electrons, can be expressed in ADU using,

$$\begin{aligned}
N_e &= gN_a && (4.7)\\
\sigma_e &= g\sigma_a && (4.8)
\end{aligned}$$

where g is the gain in electrons per ADU, N_a is the average number of electrons in ADU and the standard deviation, σ_a, is the photon noise in ADU.

Equation (4.6) becomes :

$$g^2\sigma_a^2(i) = gN_a - 2bigN_a + \mathcal{O}(b^2) \qquad (4.9)$$

or

$$\sigma_a^2(i) = \sigma_{a0}^2 - 2(1-a)\sigma_{a0}^2 i + \mathcal{O}(b^2) \qquad (4.10)$$

where σ_{a0} is the photon noise in ADU before being affected by the CTE.

In conclusion, a simple linear fit of $\sigma_a^2(i)$ versus i permits for the determination of the CTE, a.

4.3.3 Data Acquisition and Parameter Estimation

To apply the CVF method, we first need to obtain the dependance of the variance of the number of electrons on the index of the line (column). To compute this variance, two flat fields (same level of intensity) and two bias images are required. The bias images are subtracted from the flat images and the two resulting images are divided, one by the other. The final resulting image is multiplyed by the mean of the image in the denominator (see Equation (4.11)). This manipulation yields a flat-fielded image, I_f, without a fixed pattern noise (Photon Response Non Uniformity, PRNU). Using this flat-fielded image we calculate the variance (in ADU^2) which is composed of the variance of the number of electrons and the squared readout noise. I_f is given by,

$$I_f = \frac{F_1 - B_1}{F_2 - B_2} \mathcal{M}\left(F_2 - B_2\right) \tag{4.11}$$

where F_1 and F_2 are the flat field images, B_1 and B_2 are the bias images and $\mathcal{M}(F_2 - B_2)$ gives the average of all the pixels values (number of electrons in ADU) in the image $F_2 - B_2$.

The variance of the pixels values, $\sigma^2_{I_f}$, in the flat-fielded image I_f can be expressed as follows,

$$\sigma^2_{I_f} = 2\left(\sigma^2_a + \sigma^2_{ron}\right) \tag{4.12}$$

where σ_a is the photon noise (in ADU) and σ_{ron} is the readout noise (in ADU). $\sigma^2_{I_f}$ has to be divided by 2 in order to obtain the variance of the number of electrons which is present in a single frame.

We estimate the readout noise, σ_{ron}, by subtracting one bias image from the other and computing the standard deviation of the number of electrons for the resulting image. The latter has to be corrected by $\sqrt{2}$ to obtain the readout noise of a single frame,

$$\sigma_{ron} = \frac{S_d\left(B_1 - B_2\right)}{\sqrt{2}} \tag{4.13}$$

where $S_d(B_1 - B_2)$ is the standard deviation of the number of electrons (in ADU) in the image $B_1 - B_2$.

To plot the variance of the number of electrons, $\sigma^2_a(i)$, in the image I_f versus the index of line (column), i, we compute in the image I_f the variance of the pixels values in each line (column), $\sigma^2_{I_f}(i)$, and deduce from Equation (4.12) the variance of the number of electrons, $\sigma^2_a(i)$ (in ADU^2). Next a linear fit is carried out to estimate the CTE (for example see Figure 4.3).

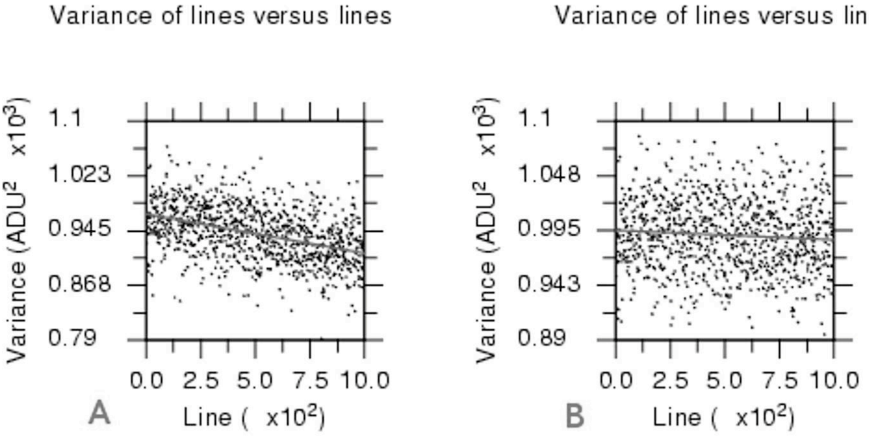

Figure 4.3: Images A and B show the plot (i, σ_a^2) at different CTEs with the best fit line in gray. In A, the CTE is 0.999970, in B, 0.999996. These plots have been done with simulated data. The average number of electrons, N_e, in each pixel of the original images is 1000 with a standard deviation of $\sqrt{1000}$ (photon statistics). The charge transfer inefficiency is applied subsequently. The dimensions of the images are 1k x 1k. Similar plots are obtained for real data.

4.3.4 Systematic Error Due to an Imperfect CTE, Impact on the Gain

Instead of working on the horizontal and vertical CTE separately, we derive the variance of the signal using both simultaneously. Equation (4.10) becomes :

$$\sigma_a^2(i,j) \quad = \quad \sigma_{a0}^2 - 2b_h\sigma_{a0}^2 i - 2b_v\sigma_{a0}^2 j + \mathcal{O}(b^2) \qquad (4.14)$$

where $\sigma_a^2(i,j)$ is the variance of the number of electrons (in ADU^2) in the pixel (i,j) and b_h and b_v are the horizontal and vertical charge transfer inefficiency, respectively.

The calculation of the variance of the signal across the chip yields the mean variance of the signal. This value can be determined with the help of equation (4.14).

$$\overline{\sigma_a^2} \quad = \quad \sigma_{a0}^2 - b_h\sigma_{a0}^2 n_h - b_v\sigma_{a0}^2 n_v \qquad (4.15)$$

where $\overline{\sigma_a^2}$ is the mean variance of the signal (in ADU^2) in the image and n_h and n_v are the dimensions of the light sensitive matrix of the CCD.

The gain of the CCD with a perfect CTE would be $g_0 = N_a/\sigma_{a0}^2$, where N_a is the average signal level in ADU and σ_{a0}^2 is the variance of the signal when the signal is not affected by a charge transfer inefficiency. In practice we determine $g_m = N_a/\overline{\sigma_a^2}$ because of the charge transfer inefficiency. To compute g_0, we have to correct for the impact of the CTE on g_m,

CTE	$g_{err}(\%)$ [2k x 4k]	$g_{err}(\%)$ [1k x 1k]
0.999999	0.6	0.2
0.999998	1.2	0.4
0.999997	1.8	0.6
0.999996	2.4	0.8
0.999995	3.0	1.0

Table 4.1: Theoretical estimate of the error in the gain due to an imperfect CTE that occurs when the photon transfer method is used to determine the gain. The errors are calculated for two ideal CCDs that are affected only by an imperfect CTE. The first one is a CCD which has 2k × 4k pixels (second column) and the second one has 1k × 1k pixels (third column).

$$\frac{g_0}{g_m} = \frac{\overline{\sigma_a^2}}{\sigma_{a0}^2} = 1 - b_h n_h - b_v n_v \tag{4.16}$$

Thus the gain of the CCD after correction is,

$$g_0 = \frac{N_a}{\overline{\sigma_a^2}} (1 - b_h n_h - b_v n_v) \tag{4.17}$$

and the systematic error in the gain produced by the CTE can be expressed as follows,

$$g_{err}\,[\%] = (b_h n_h + b_v n_v) \times 100 \tag{4.18}$$

Table 4.1 lists the theoretical estimate of the error in the gain which is expected because of the imperfect CTE when the photon transfer method is employed. The horizontal and vertical CTEs are identical in these simulations.

4.4 Results

4.4.1 Simulated Data

The CVF method has been tested on simulated data. For this purpose, images (1k × 1k pixels) with a mean intensity of 1000 e^- and a photon noise of $\sqrt{1000}$ have been generated. For each image different CTEs have been applied (see column one of Table 4.2). The procedure based on the study of the variance of the signal (developed in Section 4.3.2) is used to extract the horizontal and vertical CTE. The first test based on simulated images shows that the CVF method recovers the CTE values extremely well (Table 4.2). The computed results for the CTE are in accordance with the original values of the CTE.

Some tests have been carried out on the current simulated images to check the impact of an imperfect CTE on the gain. We used the photon transfer method to calculate this parameter (see Table 4.3, second column) and observed an increase in the gain as a function of the degradation of the CTE. Next, equation (4.17) was used to correct the

Theoretical CTE	CVF Method	
H & V CTE	H-CTE*	V-CTE*
1.0	1.0	0.999999
0.999998	0.999998	0.999998
0.999996	0.999995	0.999995
0.999994	0.999993	0.999994
0.999992	0.999992	0.999992
0.999990	0.999990	0.999990
0.999985	0.999985	0.999985
0.999980	0.999980	0.999981
0.999970	0.999971	0.999971

*Error : ± 0.000001

Table 4.2: CVF method applied to simulated data to estimate the CTEs of the CCDs. The first column lists the theoretical CTE used to generate the simulated data. Columns two and three show the horizontal and vertical CTE obtained with the CVF method using the light sensitive matrix of the CCD.

CTE	Gain		
H & V CTE	Gain measured	Gain corrected	g_{err}%
1.0	1.00272		
0.999998	1.00647	1.00244	0.4
0.999996	1.01078	1.00067	1.0
0.999994	1.01483	1.00164	1.3
0.999992	1.01888	1.00258	1.6
0.999990	1.02294	1.00248	2.0
0.999985	1.03312	1.00213	3.0
0.999980	1.04335	1.00266	3.9
0.999970	1.06396	1.00225	5.8

Table 4.3: Impact of an imperfect CTE on the gain. The different CTEs used to create 1k × 1k simulated images are listed in the first column. The second column shows the gain obtained from images affected by charge transfer inefficiency. The corrected gains are tabulated in the third column and the errors are shown in the last column. The gain in the first line of this table is used as reference. The complete light sensitive area of the CCD is used to compute the gain.

gain. We employed for b_h and b_v the CTEs that have been computed for the simulated images (see Table 4.2) and noticed that the use of equation (4.17) recovered the gain very well (see Table 4.3, third column). To estimate the error, g_{err}%, the gain obtained from flat field images, which are not affected by charge transfer inefficiency, is used as reference (see Table 4.3, first line).

4.4.2 Real Data

Data sets from 9 CCDs have been used to test the CVF method. Each set is composed of two bias images and two flat field images. Two FIERA clock modes have been employed to acquire these images. 5 sets of images have been taken with the "225 kpix/s - High Gain" mode and the other 4 have been acquired with the "225 kpix/s - Low Gain" mode, all of them at -120 degrees Celsius. High gain and low gain correspond to $\sim 0.54e^-/ADU$ and $\sim 2.5e^-/ADU$, respectively. The CVF method developed in Section 4.3.2 is used to estimate the CTE and the results are compared to the results obtained at ESO using the EPER method as well as well as to those, obtained by e2V. e2V uses the ^{55}Fe method to estimate the CTEs of the produced CCDs at -100 degrees. The results for the CTEs of the current study are tabulated in Table 4.4. The comparison shows that the CVF method estimates better the CTE than the EPER method. The values of the CTEs from the ^{55}Fe method are used as reference in this study. Almost all calculations carried out with the CVF method are consistent with the study made by e2V. The EPER method is known to overestimate the CTE (Janesick, 2001). This is so because it uses the charges that are deferred in the extended pixel region (overscan), but does not take into account defects that are present in the sensitive area of the chip.

Despite these promising results we should not ignore the differences observed for the CCDs ColumbaII and MicroscopiumII. For these two CCDs the results from the horizontal CTE computations performed using both the CVF and EPER methods are in accordance but they are not in agreement with the e2V results. The observed differences may result from traps. In flat field images the traps are filled and do not catch charges during the transfer which is not the case with images used by the ^{55}Fe method. In that case the traps catch more charges and consequently, they lower the CTE value. For CCD ColumbaII we have applied the CVF method on data using the "50 kpix/s - High Gain" mode and using images which have different signal levels ($\sim$12100 e^- and $\sim$850 e^-). We obtained for the horizontal CTE of this device similar results with a CTE of 0.999998 and 0.999997, respectively. For the CCD Telescopium, the first column of the X-overscan region has an abnormally high level of intensity. This phenomenon is observed in all flat field images of this chip and indicates a low value of the CTE. Using the EPER method we obtained a CTE value of 0.999990 whereas employing the other two techniques, CVF and ^{55}Fe, the CTE value is estimated to be larger, 0.999995 and 0.999996, respectively. The very low value of the CTE, 0.999990 obtained with the EPER method, may reflect a local defect in the x-overscan region of the chip. If the CTE, yielded by the CVF and ^{55}Fe techniques, would have been in the same range as that obtained with the EPER method, the defect would have a different nature and it would be no longer local but rather extended over the complete chip surface.

4.5 Conclusion

A new technique to compute the Charge Transfer Efficiency (CTE) of a CCD has been presented in this chapter. The imperfect charge transfer which occurs during the readout of an integrated image has a smoothing effect on the final image. The method developed above analyses the change in the variance of the number of electrons as a function of the CCD row and column in simple flat field images, caused by the smoothing effect of the imperfect charge transfer.

We tested the CVF method on simulated images (an ideal 1k x 1k CCD with only charge transfer inefficiency) and real images from the OmegaCAM CCDs. No modifications of the ESO test bench were required to carry out CTE analyses with the CVF method which is a variance-based technique. We used simple flat filed images to esti-

CCD	Horizontal CTE			Vertical CTE		
	CVF	EPER	^{55}Fe	CVF	EPER	^{55}Fe
"225 kpix/s - High Gain" mode						
Chameleon	0.999999	0.999997	0.999999	0.999998	0.999999	0.999998
Dorado	0.999998	0.999999	0.999998	0.999998	0.999999	0.999998
Fornax	0.999998	0.999999	0.999997	0.999998	0.999999	0.999997
Grus	0.999996	0.999998	0.999997	0.999999	0.999999	0.999998
Mensa	0.999998	0.999998	0.999999	0.999997	0.999999	0.999997
"225 kpix/s - Low Gain" mode						
ColumbaII	0.999997	0.999997	0.999993	0.999999	0.999999	0.999999
MicroscopiumII	0.999998	0.999997	0.999995	0.999998	0.999999	0.999999
MuscaAustralisII	0.999997	0.999998	0.999997	0.999998	0.999999	0.999998
Telescopium	0.999995	0.999990	0.999996	0.999999	0.999999	0.999998

Table 4.4: Estimate of the Horizontal and Vertical CTE of 9 CCDs using the CVF, EPER and ^{55}Fe methods.

mate the CTE. The results for the CTE, obtained from the computations carried out with simulated images, are in accordance with the theoretical CTE. To validate the CVF method on real images we compared the results for the CTE yielded by the CVF method to those, obtained by the studies performed with a ^{55}Fe setup. The calculations, based on the CVF method, yielded for the real images CTE results in accordance with those computed using a ^{55}Fe setup. In addition, the CVF method overcomes one of the major drawbacks of the ^{55}Fe based method, namely the use of a hazardous radioactive material to carry out the investigations. Compared to the EPER method, the CVF method provides better estimates of the CTEs.

The CVF method is still under development however, it has already proved reliable. The results obtained for the CTEs of the CCDs show that the CVF method can be used to estimate, with a high level of confidence, the charge transfer efficiency of CCDs. This technique, employed as a complement to the EPER method, is suitable for studies where ^{55}Fe setups can not be employed.